Insight into the contributions of primary emissions of sulfate, nitrate, and ammonium from residential solid fuels to ambient $PM_{2.5}$

Yue Zhang[1, 2], Yiming Yang[1], Leiming Zhang[3], Hongmei Xu[1]*, Jian Sun[1], Tao Wang[4], Fangxiang Li[4], Xiaojian Chang[4], Steven Sai Hang Ho[5], Bin Li[2], Bing Wang[2], Junji Cao[6], Zhenxing Shen[1, 6*]

[1] Department of Environmental Science and Engineering, Xi'an Jiaotong University, Xi'an 710049, China

[2] Key laboratory of tobacco processing, Zhengzhou Tobacco Research Institute of CNTC, Zhengzhou 450001, China

[3] Air Quality Research Division, Science and Technology Branch, Environment and Climate Change Canada, Toronto, Canada

[4]Agricultural Technology & Extension Central of Xi'an City, Xi'an 710061, China

[5]Divison of Atmospheric Sciences, Desert Research Institute, Reno, NV89512, United States

[6] The State Key Laboratory of Loess and Quaternary Geology, Institute of Earth Environment, Chinese Academy of Sciences, Xi'an, 710049, China

**Authors to whom correspondence should be addressed.*
E-mail: xuhongmei@xjtu.edu.cn (Hongmei Xu) or zxshen@mail.xjtu.edu.cn (Zhenxing Shen)

Abstract

Understanding the primary emissions of sulfate (SO_4^{2-}), nitrate (NO_3^-), and ammonium (NH_4^+) (SNA) from solid fuels (coal and biomass) combustion is important to study their roles in haze formation and particle growth. In this study, direct emissions of SNA and other inorganic ions (including Na^+, K^+, Mg^{2+}, Ca^{2+}, and Cl^-) in fine particulate matter ($PM_{2.5}$) from residential coal combustion (RCC) and biomass burning (BB) were quantified through combustion chamber experiments. Emission factors (EFs) of the total quantified ions for the five types of solid fuels are in the range of 178-3,880 mg/kg, accounting for 5.8%-41.1% of the emitted $PM_{2.5}$ mass. The average proportions of SO_4^{2-}, NO_3^-, and NH_4^+ in $PM_{2.5}$ emitted from RCC are 3.7%, 0.9%, and 1.0%, respectively, in comparison to 1.3%, 0.8%, and 0.1%, respectively, for BB. Despite the variations of SNA proportions seen among the solid fuel types, SO_4^{2-} is the most dominating inorganic ion, consistent with the emission profiles shown in other literatures. Similar mass fraction and its range of SO_4^{2-} are found between RCC and ambient in the northern cities, implying that the primary emission from RCC is a significant source contributor to atmospheric SO_4^{2-}, particularly in wintertime. According to the EFs and mass fractions of SNA determined for the solid fuels, the contribution of secondary formation to atmospheric SO_4^{2-} should be overestimated in ambient $PM_{2.5}$ source apportionment.

Keywords: $PM_{2.5}$; Sulfate; Nitrate; Ammonium; Solid Fuels; Source Identification

1. Introduction

Particulate matter (PM) has been emphasized for its impacts on both human health and climate change (Cao et al., 2012b; Fu et al., 2016; Kelly and Fussell, 2012; Shen et al., 2007; Wang et al., 2017). In 2012, the China Government promulgated the national standard of the annual average concentration of $PM_{2.5}$ (PM with an aerodynamic diameter of equal to or less than 2.5μm) of 35 $\mu g/m^3$ (Cao et al., 2012a; Kong et al., 2018). A full understanding of $PM_{2.5}$ compositions and sources is essential for establishing efficient pollution control measures (Kong et al., 2010). Ambient $PM_{2.5}$ typically consists of inorganic ions, organic carbon (OC), element carbon (EC), geological minerals, salts, trace elements, and other substances (Chow et al., 2015). The sum of inorganic ions contributed significantly to $PM_{2.5}$ in northwest China (Niu et al., 2016). Sulfate (SO_4^{2-}), nitrate (NO_3^-), and ammonium (NH_4^+) (denoted as SNA) are the three most abundant inorganic components (Shen et al., 2008).

Atmospheric SNA could be originated from both primary emissions and secondary formation. Typical primary sources include coal combustion, biomass burning, fugitive dust, industrial, and vehicular emissions (Gao et al., 2011; Shen et al., 2016; Švédová et al., 2020; Zhang et al., 2015; Zhou et al., 2016). The secondary formation of atmospheric SNA is recognized as oxidation and neutralization products from major gaseous precursors, including sulfur dioxide (SO_2), nitrogen oxides (NO_x), and ammonia (NH_3) (Wang et al., 2013; Zhang et al., 2015). The concentrations levels of SNA from the secondary formation are considered one of the main driving forces in $PM_{2.5}$ pollution (Huang et al., 2014). However, research on sulfate formation mechanisms by atmospheric chemistry models has improved our understanding of secondary sulfate, but gaps still existed between observation and model prediction in both haze and non-haze days (Wang et al., 2014). The gaps could attribute to missing sources, such as primary emissions. For example, Shen et al (2008) found that even with a much lower sulfur oxidation ratio (SOR) and similar nitrogen oxidation ratio (NOR) observed in winter compared to summer, much lower ratios of NO_3^-/SO_4^{2-} still

occurred in winter in Xi'an, northwest China, implying that the large quantities of atmospheric SO_4^{2-} directly emitted from coal combustions for heating. Dai et al. (2019) reported that primary emissions from residential coal combustion in rural Xi'an accounted for as high as 49.2% of total atmospheric SO_4^{2-} in winter. Thus, using SO_4^{2-} as a secondary formation marker in source apportionment studies could have large uncertainties, especially in the regions where solid fuels such as coal were extensively used.

To fill the knowledge gap discussed above, combustion experiments were carried out using four types of coal and one type of biomass (maize straw) that were commonly used in northwest China. Emission factors (EFs) of SNA and their proportions in $PM_{2.5}$ emitted from residential coal combustion (RCC) and biomass burning (BB) were determined. Furthermore, the results from the present study were compared with literature-reported data on the SNA proportions in $PM_{2.5}$ emitted from a variety of fuels under various combustion conditions. Contributions from primary SNA emissions to ambient $PM_{2.5}$ were finally elaborated.

2. Methods

2.1 Fuel selection and combustion tests

Four types of coals, including anthracite chunk (A-chunk), anthracite briquette (A-briquette), bituminous chunk (B-chunk), and bituminous briquette (B-briquette), and one biomass fuel of maize straw were selected as the combustion samples considering their wide applications in northwest China. The briquettes used in this study were produced following the procedures described in our previous study (Zhang et al., 2020). During the briquetting process, no additive was added to avoid the alternation of coal properties and particle emission characteristics.

The experiments were all conducted inside a regulated combustion chamber with a volume of 8 m^3. The chamber and inner surface are made with aluminum alloy and equipped with a dilution sampler which captured emitted particles from the stages of

ignition to extinction. Detailed descriptions of the chamber were shown by Sun et al. (2017) and Zhang et al. (2020). The dilution sampler can collect $PM_{2.5}$ in the diluted plume onto three 47 mm filters in parallel, including two quartz filters (Whatman, Maidstone, UK) and one Teflon filter (Pall Life Sciences, Ann Arbor, MI, USA) (Tian et al., 2015). The gravimetric measurement was conducted using an electronic balance with a sensitivity of ±1 μg (ME 5-F, Sartorius, Göttingen, Germany). All of the filters before and after the sample collection were placed in a weighing chamber at a temperature of 22±2 ℃ and relative humidity (RH) of 35%±5% for at least 24 h before weighing.

2.2 Water-soluble ions analysis

One-quarter of the quartz filter was cut, placed into a Teflon tube, and extracted with 10 ml of deionized water by mechanical shaking for 30 min, and repeated extraction three times. The combined extractant was then filtered through a 0.45 μm pore size membrane before being injected into an ion chromatography (Dionex Cooperation, Sunnyvale, CA, USA). Cations (i.e., Na^+, NH_4^+, K^+, Mg^{2+}, and Ca^{2+}) and anions (i.e., Cl^-, NO_3^-, and SO_4^{2-}) were quantified. Detailed information on the ion analytical method and its QA/QC can be found in Shen et al (2011).

2.3 Emission factors calculation

Mass-based emission factors (EFs) were calculated using the following equation (Zhang et al., 2020):

$$EF=\frac{m_{particle}\times DR\times t_{sample}\times V_{stk}\times D}{Q_{filter}\times m_{fuel}} \quad (1)$$

where $m_{particle}$ stands for the mass of particles deposited on the filter (mg), DR is the dilution rate during sampling, t_{sample} is the sampling time (from ignition to extinction); V_{stk} is the velocities of the chamber stack (m/s), D stands for the cross-sectional area of the stack (m^2); Q_{filter} is the volume of air passed through the filter (m^3), and m_{fuel} is the mass of fuel consumed in each test (kg).

3. Results and Discussion

3.1 $PM_{2.5}$ and water-soluble ions emitted from RCC and BB

Table 1 lists the EFs of $PM_{2.5}$ and the target inorganic ions for the four types of coal and one type of biomass fuel. The $PM_{2.5}$ EFs for the four coals range from 0.51±0.13 to 3.08±0.19 g/kg, much lower than that of 11.2±3.67 g/kg for maize straw (BB). The EFs of the total quantified ions range from 178-3,886 mg/kg for both solid fuels, contributing 5.8%-41.1% of the $PM_{2.5}$ mass. For the anthracite coal, the EFs of SO_4^{2-}, NO_3^-, and NH_4^+ for its chuck/briquette are 29.9±7.52/76.2±71.8, 8.86±1.46 /8.51±0.00, and 21.0±24.8/18.4±24.1 mg/kg, respectively, while for the bituminous coal, showing 27.8±3.70/36.9±19.2, 9.44±1.16/8.44±4.27, 0.04±0.06/6.47±4.00 mg/kg, respectively. Even though EFs of SO_4^{2-} and NO_3^- between the chuck and briquette for anthracite and bituminous coals are close, large discrepancies are seen for other inorganic ions. For instance, the EFs of NH_4^+ for briquette bituminous are three orders of magnitude higher than raw bituminous, demonstrating the compositions of inorganic ions could be influenced by the briquetting process. In comparison to the coals, much higher EFs of SNA are seen for maize straw, which are 108±95.0, 68.0±30.3, and 10.9±17.9 mg/kg of SO_4^{2-}, NO_3^-, and NH_4, respectively. The results demonstrate that variations in fuel types could significantly alter the EFs for SNA, and further change the contribution rate of initial emission from RCC and BB to the atmospheric occurrence, particularly during the wintertime for heating using solid fuel. Rather than SNA, the EFs of K^+ for maize straw is 2,150±1,586 mg/kg, much higher than that of other ions. It should be also noted that the EFs of K^+ for coals are approximately three orders of magnitude lower than for maize straw, which accounted for a negligible fraction of the total quantified inorganic ions. The finding is consistent with the fact that K/K^+ is a remarkable tracer for BB in source apportionment (Andreae and Merlet, 2001; Chen et al., 2017; Sun et al., 2019).

Insert Table1

3.2 Proportions of SNA in $PM_{2.5}$ emitted from solid fuels in this study and comparison with other sources in the literature

Table 2 lists the mass proportions of SNA in $PM_{2.5}$ emitted from the solid fuels of RCC and BB in this study. The average proportions of SO_4^{2-}, NO_3^-, and NH_4^+ in $PM_{2.5}$ for RCC are 4.1±3.4%, 1.1±1.0%, and 1.4±2.1%, respectively, in comparison to lower values of 1.3±1.4%, 0.8±0.5%, 0.1±0.1% for BB. The results probably represent the primary SNA emission is more predominant in RCC than BB. Furthermore, SO_4^{2-} for RCC shows the highest ion proportion in $PM_{2.5}$ (Dai et al., 2019; Shen et al., 2008), which is consistent with its high abundance in northwest China, especially during the heating season (Shen et al., 2008). It should be noted that significantly lower proportions of NH_4^+ and NO_3^- ($p<0.05$) are found for RCC, demonstrating that it is not a significant source for these two inorganic ions.

Insert Table2

Figure 1 further illustrates the proportions of SNA emitted from RCC and BB among the studies (as the data shown in Table 2) to present the range of SNA fractions in $PM_{2.5}$ for RCC and BB. The mass proportions of SNA for both RCC and BB follow the order of $SO_4^{2-} > NH_4^+ > NO_3^-$. Among those studies, the average mass proportions of SO_4^{2-}, NO_3^-, and NH_4^+ in $PM_{2.5}$ for RCC are 10.1%, 0.7%, and 2.0%, respectively, whereas lower values of 1.1%, 0.3%, and 0.3% are seen for BB. In terms of range, much smaller variations are seen for NO_3^- (0.05%-2.2%) than SO_4^{2-} (1.0%-30.0%) and NH_4^+ (0.003%-9.9%). These fractions could be largely inferred by the physical states (e.g., chunk or briquette) and coal sources (anthracite or bituminous) on the emission of SNA. For BB, the proportions of SO_4^{2-}, NO_3^-, and NH_4^+ in $PM_{2.5}$ are in ranges of 0.1%-6.9%, 0.03%-0.8%, and 0.03%-1.7%, respectively. The SNA proportions in BB $PM_{2.5}$ all show much narrower variations compared to that of RCC, which reveals that the SNA emissions are relatively much more stable from BB than from RCC. And the SNA

186 abundances in BB are relatively lower compared to that of RCC.

187

188 *Insert Figure1*

189

190 Table 2 also summarizes EFs and proportions of SNA in $PM_{2.5}$ emitted from a
191 variety of solid fuels and materials (e.g., peats, electric waste, household garbage,
192 barbeque, road dust, and construction) using different combustion devices and under
193 various combustion conditions. The EFs and proportions of NH_4^+ and NO_3^- in $PM_{2.5}$
194 emitted from open burnings of electric waste (E-waste) and household garbage burning,
195 barbeque, and dust are close to the values for RCC. However, the EFs and proportion
196 of SO_4^{2-} are much higher than those of other sources. Besides, the SNA proportions for
197 BB are similar to those of dust but far lower than those of open-burning activities.
198 Results before and after aging from peat burning reported by Chow et al. (2019)
199 was also compared. Peat is an important and common solid fuel. Its EFs and proportions
200 of SNA for five different peats collected worldwide are all lower than those of RCC
201 and BB in this study. However, after simulations of two-equivalent days of atmospheric
202 aging with an oxidation flow reactor (OFR), the proportions of NH_4^+ and NO_3^- in $PM_{2.5}$
203 emitted from peats are higher than those from BB. And after seven-equivalent days of
204 aging, the two ions are even higher than those from RCC. Eventually, the secondary
205 formations occur with their corresponding gaseous precursors (i.e., NH_3 and NO_x)
206 during the aging processes. Nevertheless, the proportions of SO_4^{2-} in $PM_{2.5}$ emitted
207 from peats are still lower than those of RCC in this study even after seven -equivalent
208 days of stimulated aging. This concludes that the secondary formation of SNA might
209 not be always more important than primary emission for a few solid fuels, particularly
210 of SO_4^{2-} in coal in this study. The limitation of its precursor (e.g., SO_2) would be a
211 dominant factor.

212 *3.3 Comparisons of SNA proportions in ambient $PM_{2.5}$*

213 Table 3 summarizes the SNA proportions in ambient $PM_{2.5}$ in the Chinese cities,

and Figure 2 compares the statistical data (i.e., average value). The range (average) proportions of SO_4^{2-}, NO_3^-, and NH_4^+ in ambient $PM_{2.5}$ are 6.1%-36.0% (19.1%), 4.8%-36.9% (15.1%), and 3.2%-19.7% (9.9%), respectively. The general order of SO_4^{2-} > NO_3^- > NH_4^+ in ambient $PM_{2.5}$ is different from those of RCC and BB (i.e., SO_4^{2-} > NH_4^+ > NO_3^-). For NH_4^+, the lowest proportion in ambient $PM_{2.5}$ is even higher than the median for RCC or BB in this study (Table 2), implying that there are other critical sources for atmospheric NH_4^+. For NO_3^-, the lowest proportion in ambient $PM_{2.5}$ is also much higher than that for RCC and BB, suggesting that primary emissions from RCC and BB are not the major contributor of NO_3^- in most Chinese cities.

The proportion of SO_4^{2-} for BB is relatively low, but a higher value is seen in ambient $PM_{2.5}$ (19.1% on average), implying that BB is not a significant source. On the contrary, it is noted that the ranges of SO_4^{2-} proportion are similar between RCC (1.0%-30.0%) and ambient $PM_{2.5}$ (6.1%-36.0%), but the medium is much lower for RCC (5.3%) than ambient $PM_{2.5}$ (17.5%). This could be explained by various pollution sources contributed to ambient SO_4^{2-}. However, the primary emission of RCC could be a major source of SO_4^{2-} in the northern cities in China, such as Lanzhou, Xi'an, Beijing, and Tianjin, which show an average mass proportion of 13.3%, consistent with the average proportion of RCC. A series of research conducted by Dai et al. (2018; 2019) proved that atmospheric sulfate in winter Xi'an was not only attributed to secondary formation. Moreover, the $PM_{2.5}$-bound sulfate is 49.2% from RCC primary emissions and 50.8% from SO_2-derived secondary sources and other primary sources in winter Xi'an. For the southern cities in China, the impacts of RCC should be much lower due to less solid fuel combustion in wintertime, but a higher proportion of SO_4^{2-} (23.0% on average), implying that more potential secondary formation occurred in this region.

Insert Figure2

Insert Table3

According to Table S1, the contribution rate (less than 1%) from BB primary emissions to ambient SNA are all negligible in either winter or summer, south or north.

For RCC primary emissions, no significant contribution rates were found for ambient nitrate as well (0.1%-3.0%). But the contribution rates to ambient ammonium (3.4%-9.3%) in northern cities in winter cannot be ignored. And RCC primary emissions significantly contributed to ambient sulfate (10.5%-26.6%) in northern cities in winter. While in southern cities, or northern cities in summer, residential coal was not widely used. Therefore, no similar results can be found.

Uncertainties do exist in our estimation and mainly originated from two sources, and uncertainties for estimated results in Table S1 should be the combination of the two sources. Source one is the uncertainty in sulfate EFs obtained from literatures that may not be harmonized when measuring the composition. Ideally, such kind of uncertainties that related to measuring methods and quality control measures should be well expressed in variations of EFs. Thus, average sulfate EFs used for estimation were 10.1 for RCC and 1.1 for BB (Fig 1), with type A uncertainties (expressed as percentages) of 24.4%, 26.4%, respectively. Source two is from meteorological conditions that affect physical process like advection and diffusion of primary air pollutants but also formation of secondary air pollutants. Due to lack of uncertainty numbers in the cited papers regarding source two, detailed estimation cannot be done here. Thus, the overall uncertainties for sulfate concentrations in Table S1 are 24.4% for RCC and 26.4% for BB, respectively. However, uncertainties from source two could also alter the estimated sulfate concentrations significantly and should be well quantified in future source apportionment studies.

4. Conclusions

EFs of primary SNA in $PM_{2.5}$ were determined for the common solid fuels used for heating in northwest China. Compared with the results in the literatures, the proportions of SNA for RCC greatly vary with different physical states and types of the coals, in addition to the stoves and combustion conditions. The emissions of SNA for BB are comparatively stable but lower than RCC. The largest variation in EFs and mass fraction is observed on the SO_4^{2-} from RCC, consistent with the contributions in

ambient $PM_{2.5}$. Primary emission from RCC could be a significant contributor to atmospheric SO_4^{2-} in northwest China, which are more impacted by RCC and high precursor gas emission from coals during the heating season with low SOR. Even though SO_4^{2-} is a dominating water-soluble ion in $PM_{2.5}$ in China in the past decades, previous studies might overestimate its contribution to secondary formation in source apportionment. The results of the present study should assist in adjusting the bias and provide more understanding of their formations as well as establishing more accurate and efficient $PM_{2.5}$ control measure in the future. This study highlights that it is importance to control the primary sulfate emissions on air quality management.

Acknowledgment

This research was supported by the Key R&D Project of Shaanxi Province, China (2022ZDLSF06-07) and the Science and Technology plan project of Xi'an city (21NYYF0041).

References

Andreae, M.O., Merlet, P., 2001. Emission of trace gases and aerosols from biomass burning. Global Biogeochem Cy 15, 955-966.

Calvo, A., Martins, V., Nunes, T., Duarte, M., Hillamo, R., Teinilä, K., Pont, V., Castro, A., Fraile, R., Tarelho, L., 2015. Residential wood combustion in two domestic devices: Relationship of different parameters throughout the combustion cycle. Atmos Environ 116, 72-82.

Cao, J. J., Shen, Z. X., Chow, J.C., Watson, J.G., Lee, S. C., Tie, X. X., Ho, K. F., Wang, G. H., Han, Y. M., 2012a. Winter and summer $PM_{2.5}$ chemical compositions in fourteen Chinese cities. J Air Waste Manage 62, 1214-1226.

Cao, J. J, Xu, H. M, Xu, Q., Chen, B. H, Kan, H. D, 2012b. Fine particulate matter constituents and cardiopulmonary mortality in a heavily polluted Chinese city. Environ Health Persp 120, 373-378.

Chen, J., Li, C., Ristovski, Z., Milic, A., Gu, Y., Islam, M.S., Wang, S., Hao, J., Zhang, H., He, C., Guo, H., Fu, H., Miljevic, B., Morawska, L., Thai, P., Lam, Y.F., Pereira, G., Ding, A., Huang, X., Dumka, U.C., 2017. A review of biomass burning: Emissions and impacts on air quality, health and climate in China. Sci Total Environ 579, 1000-1034.

Chow, J.C., Cao, J. J, Antony Chen, L.-W., Wang, X., Wang, Q., Tian, J., Ho, S.S.H., Watts, A.C., Carlson, T.B., Kohl, S.D., 2019. Changes in $PM_{2.5}$ peat combustion source profiles with atmospheric aging in an oxidation flow reactor. Atmos Meas Tech 12.

Chow, J.C., Lowenthal, D.H., Chen, L.W.A., Wang, X., Watson, J.G., 2015. Mass reconstruction methods for $PM_{2.5}$: a review. Air Qual Atmos Hlth 8, 243-263.

Chuang, H. C., Sun, J., Ni, H. Y, Tian, J., Lui, K. H., Han, Y. M, Cao, J. J, Huang, R. J., Shen, Z. X, Ho, K. F., 2019. Characterization of the chemical components and bioreactivity of fine particulate matter produced during crop-residue burning in China. Environ pollut 245, 226-234.

Dai, Q. L, Bi, X. H, Liu, B. S, Li, L. W, Ding, J., Song, W. B, Bi, S. Y, Schulze, B.C., Song, C. B, Wu, J. H, 2018. Chemical nature of $PM_{2.5}$ and PM_{10} in Xi'an, China: Insights into primary emissions and secondary particle formation. Environ Pollut 240, 155-166.

Dai, Q. L, Bi, X. H, Song, W. B, Li, T. K, Liu, B. S, Ding, J., Xu, J., Song C. B, Yang, N. W, Schulze, B.C., Feng, Y. C, Hopke, P. K, 2019. Residential coal combustion as a source of primary sulfate in Xi'an, China. Atmos Environ 196, 66-76.

Deng, X. L., Shi, C. E., Wu, B. W., Yang, Y. J., Jin, Q., Wang, H. L., Zhu, S., Yu, C., 2016. Characteristics of the water-soluble components of aerosol particles in Hefei, China. J Environ Sci 42, 32-40.

Fine, P.M., Cass, G.R., Simoneit, B.R., 2002. Chemical characterization of fine particle emissions from the fireplace combustion of woods grown in the southern United States. Environ Sci Technol 36, 1442-1451.

Fine, P.M., Cass, G.R., Simoneit, B.R., 2004. Chemical characterization of fine particle emissions from the wood stove combustion of prevalent United States tree species. Environ Eng Sci 21, 705-721.

Fu, Y., Tai, A.P., Liao, H., 2016. Impacts of historical climate and land cover changes on fine particulate matter ($PM_{2.5}$) air quality in East Asia between 1980 and 2010. Atmos Chem Phys 16.

Gao, X., Yang, L., Cheng, S., Gao, R., Zhou, Y., Xue, L., Shou, Y., Wang, J., Wang, X., Nie, W., 2011. Semi-continuous measurement of water-soluble ions in $PM_{2.5}$ in Jinan, China: temporal variations and source apportionments. Atmos Environ 45, 6048-6056.

Hua, Y., Cheng, Z., Wang, S. X, Jiang, J. K, Chen, D. R, Cai, S. Y, Fu, X., Fu, Q. Y, Chen, C. H, Xu, B. Y, 2015. Characteristics and source apportionment of $PM_{2.5}$ during a fall heavy haze episode in the Yangtze River Delta of China. Atmos Environ 123, 380-391.

Huang, R. J., Zhang, Y. L, Bozzetti, C., Ho, K. F., Cao, J. J., Han, Y. M, Daellenbach, K.R., Slowik, J.G., Platt, S.M., Canonaco, F., 2014. High secondary aerosol contribution to particulate pollution during haze events in China. Nature 514, 218-222.

Kelly, F.J., Fussell, J.C., 2012. Size, source and chemical composition as determinants

of toxicity attributable to ambient particulate matter. Atmos Environ 60, 504-526.
Kong, S. F, Han, B, Bai, Z. P, Chen, L, Shi, J. W, Xu, Z., 2010. Receptor modeling of $PM_{2.5}$, PM_{10} and TSP in different seasons and long-range transport analysis at a coastal site of Tianjin, China. Sci Total Environ, 400, 4681-4694.
Kong, S. F, Yan, Q, Zheng, H, Liu, H. B, Wang, W, Zheng, S. R, Yang, G. W, Zheng, M. M, Wu, J, Qi, S. H, Shen, G. F, Tang, L. L, Yin, Y., 2018. Substantial reductions in ambient PAHs pollution and lives saved as a co-benefit of effective long-term $PM_{2.5}$ pollution controls. Environ Int, 114, 266-279.
Ni, H. Y, Tian, J., Wang, X. L, Wang, Q. Y, Han, Y. M, Cao, J. J, Long, X., Chen, L.-W.A., Chow, J.C., Watson, J.G., 2017. $PM_{2.5}$ emissions and source profiles from open burning of crop residues. Atmos Environ 169, 229-237.
Niu, X. Y, Cao, J. J, Shen, Z. X, Ho, S.S.H., Tie, X. X. , Zhao, S. Y, Xu, H. M, Zhang, T., Huang, R. J, 2016. $PM_{2.5}$ from the Guanzhong Plain: Chemical composition and implications for emission reductions. Atmos Environ 147, 458-469.
Pinder, R.W., Adams, P.J., Pandis, S.N., 2007. Ammonia Emission Controls as a Cost-Effective Strategy for Reducing Atmospheric Particulate Matter in the Eastern United States. Environ Sci Technol 41, 380-386.
Qiao, B. Q, Chen, Y., Tian, M., Wang, H. B, Yang, F. M, Shi, G. M, Zhang, L. M, Peng, C., Luo, Q., Ding, S. M, 2019. Characterization of water soluble inorganic ions and their evolution processes during $PM_{2.5}$ pollution episodes in a small city in southwest China. Sci Total Environ 650, 2605-2613.
Shen, G. F, Tao, S., Chen, Y. C, Zhang, Y. Y, Wei, S. Y, Xue, M., Wang, B., Wang, R., Lu, Y., Li, W., 2013. Emission characteristics for polycyclic aromatic hydrocarbons from solid fuels burned in domestic stoves in rural China. Environ Sci Technol 47, 14485-14494.
Shen, Z. X, Arimoto, R., Cao, J. J, Zhang, R. J, Li, X. X, Du, N., Okuda, T., Nakao, S., Tanaka, S., 2008. Seasonal variations and evidence for the effectiveness of pollution controls on water-soluble inorganic species in total suspended particulates and fine particulate matter from Xi'an, China. J Air Waste Manage 58, 1560-1570.
Shen, Z. X, Cao, J. J, Arimoto, R., Zhang, R. J, Jie, D. M, Liu, S. X, Zhu, C. S, 2007. Chemical composition and source characterization of spring aerosol over Horqin sand land in northeastern China. J Geophys Res-Atmos 112.
Shen, Z. X, Cao, J. J, Liu, S. X, Zhu, C. S, Wang, X., Zhang, T., Xu, H. M, Hu, T. F, 2011. Chemical composition of PM_{10} and $PM_{2.5}$ collected at ground level and 100 meters during a strong winter-time pollution episode in Xi'an, China. J Air Waste Manage 61, 1150-1159.
Shen, Z. X, Sun, J., Cao, J. J, Zhang, L. M, Zhang, Q., Lei, Y. L, Gao, J. J, Huang, R. J., Liu, S. X, Huang, Y., Zhu, C. S, Xu, H. M, Zheng, C. L, Liu, P. P, Xue, Z. G, 2016. Chemical profiles of urban fugitive dust $PM_{2.5}$ samples in Northern Chinese cities. Sci Total Environ 569-570, 619-626.
Sun, J., Shen, Z. X, Cao, J. J, Zhang, L. M, Wu, T. T, Zhang, Q., Yin, X. L, Lei, Y. L,

Huang, Y., Huang, R. J, 2017. Particulate matters emitted from maize straw burning for winter heating in rural areas in Guanzhong Plain, China: current emission and future reduction. Atmos Res 184, 66-76.

Sun, J., Shen, Z. X, Zhang, Y., Zhang, Q., Lei, Y. L, Huang, Y., Niu, X. Y, Xu, H. M, Cao, J. J, Ho, S.S.H., 2019. Characterization of $PM_{2.5}$ source profiles from typical biomass burning of maize straw, wheat straw, wood branch, and their processed products (briquette and charcoal) in China. Atmos Environ 205, 36-45.

Sun, J., Shen, Z. X, Zhang, L. M, Lei, Y. L, Gong, X. S, Zhang, Q, Zhang, T, Xu, H. M, Cui, S, Wang, Q. Y, Cao, J. J, Tao, J, Zhang, N. N, Zhang, R. J., 2019. Chemical source profiles of urban fugitive dust $PM_{2.5}$ samples from 21 cities across China, Sci Total Environ 649, 1045-1053.

Sun, J, Yu, J. J, Shen, Z. X, Niu, X. Y, Wang, D. W, Wang, X, Xu, H. M, Chuang, H. C, Cao, J. J, Ho, K. F., 2021. Oxidative stress–inducing effects of various urban $PM_{2.5}$ road dust on human lung epithelial cells among 10 Chinese megacities. Ecotox Environ Safe 224, 112680.

Švédová, B., Raclavská, H., Kucbel, M., Růžičková, J., Raclavský, K., Koliba, M., Juchelková, D., 2020. Concentration Variability of Water-Soluble Ions during the Acceptable and Exceeded Pollution in an Industrial Region. Int J Env Res Pub He 17, 3447.

Tan, J. H, Zhang, L. M, Zhou, X. M, Duan, J. C, Li, Y., Hu, J. N, He, K. B, 2017. Chemical characteristics and source apportionment of $PM_{2.5}$ in Lanzhou, China. Sci Total Environ 601, 1743-1752.

Tao, J., Zhang, L. M, Zhang, R. J, Wu, Y. F, Zhang, Z. S, Zhang, X. L, Tang, Y. X, Cao, J. J, Zhang, Y. H, 2016. Uncertainty assessment of source attribution of $PM_{2.5}$ and its water-soluble organic carbon content using different biomass burning tracers in positive matrix factorization analysis—A case study in Beijing, China. Sci Total Environ 543, 326-335.

Tian, J., Chow, J.C., Cao, J. J, Han, Y. M, Ni, H. Y, Chen, L.-W.A., Wang, X. L, Huang, R. J, Moosmüller, H., Watson, J.G., 2015. A biomass combustion chamber: design, evaluation, and a case study of wheat straw combustion emission tests. Aerosol Air Qual. Res 15, 2104-2114.

Tian, J., Ni, H. Y, Han, Y. M, Shen, Z. X, Wang, Q. Y, Long, X., Zhang, Y., Cao, J. J, 2018. Primary $PM_{2.5}$ and trace gas emissions from residential coal combustion: assessing semi-coke briquette for emission reduction in the Beijing-Tianjin-Hebei region, China. Atmos Environ 191, 378-386.

Tsimpidi, A.P., Karydis, V.A., Pandis, S.N., 2008. Response of fine particulate matter to emission changes of oxides of nitrogen and anthropogenic volatile organic compounds in the Eastern United States. J Air Waste Manage 58, 1463-1473.

Wang, J. H, Niu, X. Y, Sun, J., Zhang, Y., Zhang, T., Shen, Z. X, Zhang, Q., Xu, H. M, Li, X. X, Zhang, R., 2020. Source profiles of $PM_{2.5}$ emitted from four typical open burning sources and its cytotoxicity to vascular smooth muscle cells. Sci Total Environ 715, 136949.

Wang, P., Cao, J. J., Shen, Z. X., Han, Y. M., Lee, S. C., Huang, Y., Zhu, C. S., Wang, Q. Y., Xu, H. M., Huang, R. J., 2015. Spatial and seasonal variations of $PM_{2.5}$ mass and species during 2010 in Xi'an, China. Sci Total Environ 508, 477-487.

Wang, Q. Y., Wang, Z. L., Zhang, H., 2017. Impact of anthropogenic aerosols from global, East Asian, and non-East Asian sources on East Asian summer monsoon system. Atmos Res 183, 224-236.

Wang, Y., Zhang, Q. Q., He, K., Zhang, Q., Chai, L., 2013. Sulfate-nitrate-ammonium aerosols over China: response to 2000-2015 emission changes of sulfur dioxide, nitrogen oxides, and ammonia. Atmos Chem Phys 13, 2635.

Wang, Y., Zhang, Q., Jiang, J., Zhou, W., Wang, B., He, K., Duan, F., Zhang, Q., Philip, S., Xie, Y., 2014. Enhanced sulfate formation during China's severe winter haze episode in January 2013 missing from current models. J Geophys Res-Atmos 119(17), 10-425.

Watson, J.G., Chow, J.C., Houck, J.E., 2001. $PM_{2.5}$ chemical source profiles for vehicle exhaust, vegetative burning, geological material, and coal burning in Northwestern Colorado during 1995. Chemosphere 43, 1141-1151.

Xie, Y. J, Lu, H. B, Yi, A. J, Zhang, Z. Y, Zheng, N. J, Fang, X. Z, Xiao, H. Y, 2020. Characterization and source analysis of water–soluble ions in $PM_{2.5}$ at a background site in Central China. Atmos Res 239, 104881.

Xu, J. S., Xu, M. X., Snape, C., He, J., Behera, S.N., Xu, H. H., Ji, D. S., Wang, C. J., Yu, H., Xiao, H., 2017. Temporal and spatial variation in major ion chemistry and source identification of secondary inorganic aerosols in Northern Zhejiang Province, China. Chemosphere 179, 316-330.

Yan, Q., Kong, S. F, liu, H. B, Wang, W., Wu, J., Zheng, M. M, Zheng, S. R, Yang, G. W, Wu, F. Q, 2017. Emission inventory of water soluble ions in fine particles from residential coal burning in China and implication for emission reduction (in Chinese). China Environmental Science 10, 3708-3721.

Yan, Q., Kong, S. F, Yan, Y. Y, Liu, H. B, Wang, W., Chen, K., Yin, Y., Zheng, H., Wu, J., Yao, L. Q, 2020. Emission and simulation of primary fine and submicron particles and water-soluble ions from domestic coal combustion in China. Atmos Environ, 117308.

Young, L. H., Li, C. H., Lin, M. Y., Hwang, B. F., Hsu, H. T., Chen, Y. C., Jung, C. R., Chen, K. C., Cheng, D. H., Wang, V. S., 2016. Field performance of a semi-continuous monitor for ambient $PM_{2.5}$ water-soluble inorganic ions and gases at a suburban site. Atmos Environ 144, 376-388.

Zhang, F., Wang, Z. W., Cheng, H. R., Lv, X. P., Gong, W., Wang, X. M., Zhang, G., 2015. Seasonal variations and chemical characteristics of $PM_{2.5}$ in Wuhan, central China. Sci Total Environ 518, 97-105.

Zhang, H., Wang, S., Hao, J., Wan, L., Jiang, J., Zhang, M., Mestl, H.E., Alnes, L.W., Aunan, K., Mellouki, A.W., 2012. Chemical and size characterization of particles emitted from the burning of coal and wood in rural households in Guizhou, China. Atmos Environ 51, 94-99.

Zhang, Y., Shen, Z. X, Zhang, B., Sun, J., Zhang, L. M, Zhang, T., Xu, H. M, Bei, N. F, Tian, J., Wang, Q. Y, Cao, J. J, 2020. Emission reduction effect on $PM_{2.5}$, SO_2 and NO_x by using red mud as additive in clean coal briquetting. Atmos Environ 223, 117203.

Zhou, J. B, Xing, Z. Y, Deng, J. J, Du, K., 2016. Characterizing and sourcing ambient $PM_{2.5}$ over key emission regions in China I: Water-soluble ions and carbonaceous fractions. Atmos Environ 135, 20-30.

Figure Captions

Figure 1. A summary of SNA proportions in $PM_{2.5}$ emitted from RCC and BB in literatures (black point) and this study (red point). The box plot represents the 25^{th} and 75^{th} percentile, and the lower and upper whiskers represent the lowest and highest values. Solid circles and solid triangles represent the average value and median value, respectively, for each proportion.

Figure 2. SNA proportions obtained from ambient studies. Box plot represent the 25^{th} and 75^{th} percentile and lower and upper whiskers represent lowest and highest values. Solid circle and solid triangle represent the average value and median value for each kind of proportions.

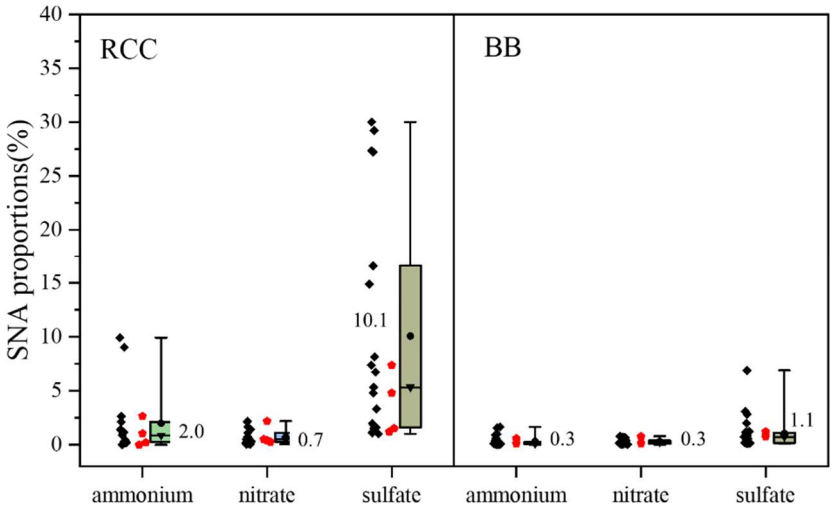

Figure 1. A summary of SNA proportions in $PM_{2.5}$ emitted from RCC and BB in literatures (black point) and this study (red point). The box plot represents the 25th and 75th percentile, and the lower and upper whiskers represent the lowest and highest values. Solid circles and solid triangles represent the average value and median value, respectively, for each proportion.

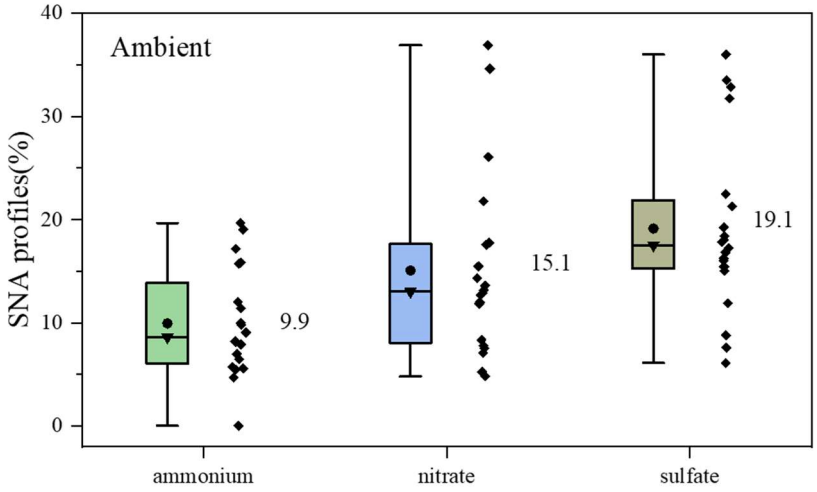

Figure 2. A summary of SNA proportions in ambient $PM_{2.5}$ from literature. The box plot represents the 25th and 75th percentile, and the lower and upper whiskers represent the lowest and highest values. Solid circles and solid triangles represent the average value and median value, respectively, for each proportion.

503 Table 1. EFs of $PM_{2.5}$, OC, EC, water-soluble ions, and elements from residential coal
504 combustion and biomass burning obtained in this study; and the results of fuel
505 proximate analysis

Component	Solid Fuels*				
	A-chunk	A-briquette	B-chunk	B-briquette	Maize straw
	Unit: g/kg				
$PM_{2.5}$	0.51±0.13	1.40±0.57	2.35±0.87	3.08±0.19	11.2±3.67
	Unit: mg/kg				
Na^+	61.2±27.4	52.9±21.6	100.8±1.59	54.6±6.98	525±209
NH_4^+	21.0±24.8	18.4±24.1	0.04±0.06	6.47±4.00	10.9±17.9
K^+	2.77±1.86	1.96±0.06	2.82±0.11	3.48±2.18	2150±1586
Mg^{2+}	6.57±4.15	6.08±5.03	13.8±0.05	4.53±0.91	95.8±62.9
Ca^{2+}	41.8±10.1	57.6±34.2	116.6±20.2	51.8±15.7	638±244
Cl^-	37.5±35.2	64.1±61.7	17.9±0.75	11.9±3.81	290±228
NO_3^-	8.86±1.46	8.51±0.00	9.44±1.16	8.44±4.27	68.0±30.3
SO_4^{2-}	29.9±7.52	76.2±71.8	27.8±3.70	36.9±19.2	108±95.0
∑ions	210±112	286±219	289±27.7	178±57.1	3886±2474
∑ions/$PM_{2.5}$ (%)	41.1	20.4	12.3	5.8	34.7
Moisture (%)	0.4	1.2	9.2	6.5	6.1
Ash (%)	8.6	7.9	3.5	4.8	4.7
Volatile matter (%)	7.3	10.1	25.7	31.2	76.0

506 * A-chunk and A-briquette represent anthracite chunk coal and anthracite briquette coal, respectively;
507 B-chunk and B-briquette represent bituminous chunk coal and bituminous briquette coal, respectively

Table 2. EFs of $PM_{2.5}$, SO_4^{2-}, NO_3^-, NH_4^+ and the ion proportions to $PM_{2.5}$ for different solid fuels obtained in this and other studies

	EFs (g/kg)	EFs (mg/kg) /proportion in $PM_{2.5}$ (%)			
*Fuel/Combustion style	$PM_{2.5}$	NH_4^+	NO_3^-	SO_4^{2-}	Reference
Coal					
A-chunk/TS	0.51±0.13	21.0±24.8 / 2.7±3.3	8.86±1.46 / 2.2±0.7	29.9±7.52 / 7.4±2.8	This study
A-briquette/TS	1.40±0.6	18.4±24.1 / 1.1±1.3	8.51±1.13 / 0.4±0.6	76.2±71.8 / 4.8±3.2	
B-chunk/TS	2.35±0.87	0.04±0.06 / 0.003±0.005	9.44±1.16 / 0.5±0.3	27.8±3.7 / 1.5±0.7	
B-briquette/TS	3.08±0.19	6.47±4.00 / 0.2±0.1	8.44±4.27 / 0.3±0.2	36.9±19.2 / 1.2±0.7	
Coal/TS	ND	ND / 1.4±1.3	ND / 0.3±0.3	ND / 3.3±2.8	(Watson et al., 2001)
A-briquette/TS	ND	ND / 9.0±3.8	ND / 1.7±1.2	ND / 6.7±3.7	(Zhang et al., 2012)
Semi coke/TS	0.75±0.19	ND / ND	3.89±0.77 / 0.5	204±83 / 27.2	(Tian et al., 2018)
B-chunk/TS	11.1±8.13	ND / ND	84.3±22.7 / 0.8	204±74 / 1.8	
A-chunk/TS	0.45±0.09	ND / ND	9.55±1.09 / 2.1	123±54 / 27.3	
A-briquette/TS	1.21±0.44	ND / ND	17.4±4.77 / 1.4	363±162 / 30.0	
A-briquette/TS	2.95	ND / 2.1±0.0	ND / 0.39±0.02	ND / 16.6±5.7	(Dai et al., 2019)
B-chunk/TS	8.58	ND / 9.9±0.5	ND / 1.12±0.2	ND / 29.2±6.6	
[a]Honeycomb-1/TS	4.88	11.59 / 0.2	4.96 / 0.1	53.45 / 1.1	(Yan et al., 2020)
[a]Honeycomb-2/TS	12.5	53.9 / 0.4	6.06 / 0.1	129 / 1.0	
[a]Honeycomb-3/TS	2.84	25.0 / 0.9	1.49 / 0.1	56.6 / 2.0	
[a]A-chunk/TS	0.39	4.52 / 1.2	2.25 / 0.6	20.8 / 5.3	
[a]B-chunk/TS	5.12	15.9 / 0.3	9.09 / 0.2	82.8 / 1.6	
[a]Honeycomb/TS	3.32±2.43	8.9±3.8 / 0.3	10.9±7.2 / 0.3	494±269 / 14.9	(Yan et al., 2017)
[a]A-chunk/TS	1.29±0.64	2.3±4.0 / 0.2	8.3±5.1 / 0.6	105±5.1 / 8.1	
Biomass					
Maize straw/TS	11.2±3.67	10.9±17.9 / 0.1±0.1	68.0±30.2 / 0.8±0.5	108±95.0 / 1.3±1.4	This study
[a]Maize straw/HK	46.1±1.4	201 / 0.4	324 / 0.7	536 / 1.2	(Sun et al., 2017)
Wheat straw/IS	9.93±0.34	60.2±11.9 / 0.6±0.1	17.9±2.98 / 0.2±0.0	72.0±12.0 / 0.7±0.1	(Sun et al., 2019b)
Wood branch/IS	1.59±0.20	2.05±0.78 / 0.1±0.1	1.41±0.56 / 0.1±0.0	14.3±2.96 / 0.9±0.2	
Wood/TS	ND	ND / 0.1±0.0	ND / 0.1±0.0	ND / 0.9±0.4	(Watson et al., 2001)
Red Maple/TS	0.88±0.16	ND / 0.2±0.0	ND / 0.7±0.1	ND / 0.6±0.1	(Fine et al., 2004)
White Oak/TS	3.4±0.5	ND / 0.1±0.0	ND / 0.4±0.0	ND / 1.0±0.0	
Loblolly Pine/TS	2.0±0.3	ND / 0.3±0.0	ND / 0.2±0.1	ND / 0.2±0.0	
[a]Q. pyrenaica/TS	13.4±3.8	14.4±1.5 / 0.1	17.1±2.2 / 0.1	16.8±7.7 / 0.1	(Calvo et al., 2015)
[a]P. nigra/TS	4.4±1.4	2.7±1.5 / 0.1	12.1±0.55 / 0.3	47.8±9.9 / 1.1	
[a]F. sylvatica/TS	2.82±0.70	2.78±0.44 / 0.1	7.1±1.9 / 0.3	8.2±2.3 / 0.3	
[a]Q. pyrenaica/open	12.5±4.1	9.8±4.9 / 0.1	13.5±1.3 / 0.1	16.9±4.1 / 0.1	
[a]P. nigra/open	14.0±5.1	4.8±1.3 / 0.0	7.6±1.3 / 0.1	23.2±4.0 / 0.2	

[a]F. sylvatica/open	5.8±1.3	2.21±0.40 / 0.0	10.4±0.46 / 0.1	14.8±3.0 / 0.3	
Forest fire/open	ND	ND/ 0.1±0.1	ND/ 0.0±0.0	ND/ 0.1±0.1	(Watson et al., 2001)
Yellow Poplar/open	6.8±0.8	ND / 0.0±0.0	ND / 0.3±0.0	ND / 0.4±0.0	(Fine et al., 2002)
White Ash/open	3.3±0.3	ND / 0.1±0.0	ND / 0.7±0.0	ND / 0.8±0.1	
Sweetgum/open	3.5±0.4	ND / 0.1±0.0	ND / 0.6±0.0	ND / 0.5±0.0	
Mockernut Hickory/open	6.8±0.9	ND / 0.1±0.0	ND / 0.3±0.0	ND / 0.2±0.0	
Loblolly Pine/open	3.7±0.4	ND / 0.1±0.0	ND / 0.3±0.0	ND / 0.2±0.0	
Slash Pine/open	1.6±0.3	ND / 0.2±0.0	ND / 0.4±0.1	ND / 1.1±0.1	
[a]Wheat straw/open	11.4±4.9	180±90 / 1.6	22±11 / 0.2	86±79 / 0.8	(Ni et al., 2017)
[a]Rice Straw/open	8.5±6.7	140±100 / 1.7	29±15 / 0.3	240±160 / 2.8	
[a]Corn straw/open	12.0±5.4	120±120 / 1.0	21±12 / 0.2	240±70 / 2.0	
[a]Sugarcane straw/open	ND	ND / 0.0	ND / 0.1	ND / 6.9	(Chuang et al., 2019)
[a]Sorghum straw/open	ND	ND / 0.9	ND / 0.7	ND / 3.1	
Other sources					
[b]Odintsovo peat (P)/open	ND	ND / 0.1	ND / 0.2	ND / 0.2	(Chow et al., 2019)
Odintsovo peat (A-2)/open	ND	ND / 1.1±0.9	ND / 0.7±0.1	ND / 0.7±0.5	
Odintsovo peat (A-7)/open	ND	ND / 3.4±1.4	ND / 2.0±0.7	ND / 0.8±0.2	
[b]Malaysia peat (P)/open	ND	ND / 0.0	ND / 0.1	ND / 0.2	
Malaysia peat (A-2)/open	ND	ND / 0.8±0.1	ND / 0.9±0.2	ND / 0.6±0.2	
Malaysia peat (A-7)/open	ND	ND / 4.7±0.8	ND / 4.7±1.3	ND / 2.0±0.1	
Electric waste/open	25.4±17.0	ND / 0.6±1.0	ND / 0.1±0.1	ND / 2.5±1.6	(Wang et al., 2020)
Household garbage/open	18.4±9.78	ND / 2.3±0.1	ND / 0.7±0.1	ND / 1.4±0.3	
Barbeque/open	16.8±1.87	ND / ND	ND / 1.0±0.9	ND / 3.4±2.8	
[a]Road dust	ND	ND / ND	ND / 0.4	ND / 1.7	(Shen et al., 2016)
[a]Construction dust	ND	ND / ND	ND / 0.3	ND / 1.5	
Road dust	ND	ND / ND	ND / 0.2	ND / 1.3	(Sun et al., 2019)
Construction dust	ND	ND / ND	ND / 0.2	ND / 1.2	
Road dust-Downtown	ND	ND / 0.02	ND / 0.6	ND / 1.2	(Sun et al., 2021)
Road dust-Non downtown	ND	ND / 0.03	ND / 0.2	ND / 0.8	

[*] EFs are expressed in three significant digits; proportions are expressed in one decimal place, and "ND" denotes no data available in the cited literature; "TS" denotes "Traditional Stoves"; "HK denotes "Heated Kang", "IS" denotes "Improved Stoves".

[a] Proportions were calculated using the EFs for the ions and $PM_{2.5}$ obtained in the corresponding literature.

[b] The average value accounted for all primary proportions shown in the literature.

515 Table 3. Ambient mass concentrations of $PM_{2.5}$, SO_4^{2-}, NO_3^-, and NH_4^+ in selected
516 Chinese cities

City	Season	Conc (μg/m^3)				
		$PM_{2.5}$	NH_4^+	NO_3^-	SO_4^{2-}	References
Xi'an (urban)	Annual	167	9.13	19.8	25.8	(Wang et al., 2015)
Xi'an (rural)	Annual	90.2	6.30	14.0	17.4	(Wang et al., 2015)
Xi'an	Winter	345	16.2	24.5	26.2	(Huang et al., 2014)
Beijing	Winter	159	15.6	19.1	25.4	(Huang et al., 2014)
Lanzhou	Winter	182	11.7	14.1	16.0	(Tan et al., 2017)
Shanghai	Winter	91.0	7.46	12.4	10.8	(Huang et al., 2014)
Guangzhou	Winter	69.0	6.90	8.90	12.7	(Huang et al., 2014)
Nanjing	Winter	63.0	12.0	21.8	20.7	(Hua et al., 2015)
Suzhou	Winter	99.0	17.0	25.8	31.4	(Hua et al., 2015)
Tianjin and Wuqing	Annual	149	8.50	19.6	24.2	(Zhou et al., 2016)
Zhejiang and Haining	Annual	110	6.10	13.9	16.5	(Zhou et al., 2016)
Taichung, Taiwan	Annual	21.0	4.13	4.57	7.56	(Young et al., 2016)
Beijing	Summer	138	10.9	11.5	23.2	(Tao et al., 2016)
Beijing	Winter	139	4.5	7.3	8.5	(Tao et al., 2016)
Hangzhou	Annual	80.0	9.10	14.2	13.8	(Xu et al., 2017)
Hefei	Annual	86.3	7.82	15.1	15.56	(Deng et al., 2016)
Chongqing (urban)	Summer	47.9	3.90	2.30	10.2	(Qiao et al., 2019)
Chongqing (urban)	Winter	90.7	10.9	13.0	20.4	(Qiao et al., 2019)
Wuhan	Average of Jun to Aug	25.6	4.02	1.92	8.57	(Xie et al., 2020)
Wuhan	Average of Dec to Feb	66.0	10.4	24.3	11.8	(Xie et al., 2020)

517 ** Concentrations are expressed in three significant digits; proportions are expressed in one decimal place.